American Mineralogist, Volume 81, pages 891–901, 1996

# Cathodoluminescence of quartz from sandstones: Interpretation of the UV range by determination of trace element distributions and fluid-inclusion *P-T-X* properties in authigenic quartz

CHRISTELLE DEMARS,[1,*] MAURICE PAGEL,[1] ETIENNE DELOULE,[2] AND PHILIPPE BLANC[3]

[1]CREGU and G.R. CNRS-CREGU, B.P. 23, 54501 Vandoeuvre-les-Nancy Cedex, France
[2]CNRS-CRPG, B.P. 20, 54501 Vandoeuvre-les-Nancy Cedex, France
[3]Service MEB, URA CNRS 1761, Département de géologie sédimentaire, case 104, Université P. et M. Curie, 75252 Paris Cedex 05, France

## ABSTRACT

Quartz overgrowths from Keuper sandstones of the Paris basin were examined using cathodoluminescence (CL) microscopy and spectroscopy coupled with a scanning electron microscope (SEM). With the use of standard cold CL equipment, it was observed that the emission of authigenic quartz is much less intense than that of detrital quartz grains, but a reversal of intensity was observed with scanned CL in the 200–800 nm range. The main CL emission band of diagenetic quartz is at 330–340 nm in the UV range, with other bands in the visible range. The determination of trace element distributions in authigenic quartz by in situ analyses and by SIMS imagery reveals the correlation of the 330–340 nm emission band with the highest Al and Li contents. The cathodoluminescence emission of diagenetic quartz in the UV range appears to be influenced by the coupled substitution of Al and Li into the crystal. Two explanations are suggested: (1) Al, Li, or both serve as activators, and (2) the incorporation of Al and Li causes lattice defects that lead to an enhancement of the intrinsic luminescence. Trace element analyses and fluid-inclusion studies revealed that quartz overgrowths precipitated from a fluid that partially originated from an Li-enriched primary brine derived from eastern Triassic evaporites of the Paris basin. The specific CL emission band in the UV range can be linked to the diagenetic environment. The chemistry of the fluids appears to be the essential parameter, whereas precipitation temperatures do not influence the occurrence of such emissions.

## INTRODUCTION

The cathodoluminescence (CL) technique allows the differentiation of diagenetic overgrowths from detrital quartz grains (Smith and Stenstrom 1965; Sippel 1968). Cathodoluminescence has been extensively used in sandstone diagenetic studies because of the different CL properties of authigenic and detrital quartz (Ruppert et al. 1985; Marshall 1988; Burley et al. 1989; Hogg et al. 1992; Guscott and Burley 1993). Nevertheless, the factors responsible for the CL properties of quartz are still debated (Hanusiak 1975; Zinkernagel 1978; Sprunt 1981; Owen 1984; Ramseyer and Mullis 1990; Perny et al. 1992). The study of quartz overgrowths from Keuper sandstones of the Paris basin provides an opportunity to investigate the CL characteristics of quartz from geologic samples by combining CL spectra and trace element analyses. The purpose of this work is (1) to determine the occurrence of quartz overgrowths in Keuper sandstones of the Paris basin with the use of CL, (2) to supplement visual microscopic examination of CL with spectral analyses, (3) to search for possible correlations between trace element contents and specific CL occurrence in quartz overgrowths, and (4) to discuss a possible correlation between this CL occurrence and the diagenetic environment of quartz precipitation by comparing the CL characteristics of Paris basin quartz overgrowths with those of North Sea (Alwyn area) quartz overgrowths. Quantitative in situ trace element determinations in the parts per million range were obtained with the use of secondary ion mass spectrometry (SIMS) (Shimizu et al. 1978) with the aim of resolving the origin of the observed CL. Incorporation of trace elements such as Al, Fe, Ti, Li, Na, and K in quartz crystals is well known (Bambauer 1961; Suttner and Leininger 1972; Smith and Steele 1984; among others). Their heterogeneous distribution reflects the physical-chemical variations of the fluids during crystal growth (Ramseyer and Mullis 1990). Determination of changes in trace element contents allows detection of variations of the crystal-growth conditions. The study of trace element distribution may also contribute to an understand-

* Present address: Total CST, Route de Versailles 78470 St. Remy les Chevreuse, France.

0003-004X/96/0708-0891$05.00

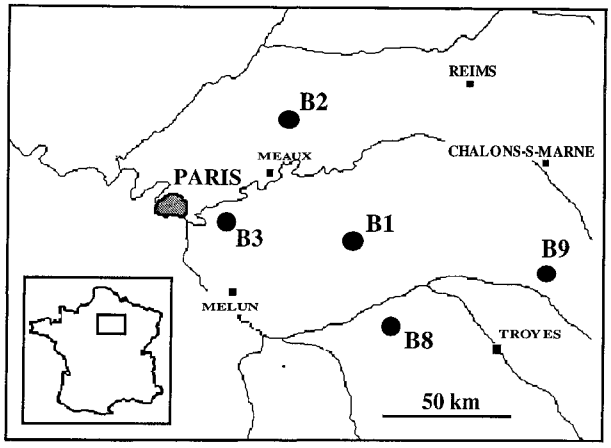


FIGURE 1. Study area and borehole location in the Paris basin (France).

ing of CL intensity. Mn was included among the elements analyzed because it has been mentioned as a possible CL activator (Marshall 1988). H was also analyzed to investigate the possible effect of $H_2O$ on CL (Owen 1984). The nature of the precipitating fluids was determined by fluid-inclusion microthermometry, which allows a better understanding of the type of diagenetic quartz studied.

## THE KEUPER SANDSTONES OF THE PARIS BASIN

The Paris basin is an intracratonic basin in north central France, filled with Triassic to Tertiary sediments with a maximum thickness of 3000 m. Four stratigraphic levels have oil-reservoir characteristics: the Keuper, the Rhaetian, and the Neocomian sandstones, and the Bathonian-Lower Callovian limestones. The samples described here were collected in the Keuper stratigraphic level, except for one sample, which belongs to the Rhaetian reservoir. About 20 samples from the Keuper units were collected from boreholes B1, B2, B3, and B8 (Fig. 1) at depths ranging from 2600 to 2800 m, and the Rhaetian sample was collected from borehole B9 at a depth of 2000 m. All the samples were observed using CL-SEM; seven samples were used for spectral analyses.

The Keuper reservoirs consist mainly of fluvial sandstones (Chaunoy and Donnemarie deposits in the western part), dolomites (Spötl et al. 1993), and some clay-rich units, which are associated with evaporite, especially anhydrite in the eastern part of the basin. The Keuper sandstones studied are principally lithic arkose with some lithic subarkose and feldspathic litharenite according to McBride's (1963) classification.

The main cement is dolomite (up to 35% determined by point counting) except in the eastern boreholes where dolomite is rare and associated with a large amount of anhydrite cement (up to 27% in borehole 8). Conventional and CL petrographic studies have revealed several generations of dolomite that occur as zoned crystals. Quartz cements are also present as overgrowths around detrital quartz grains (up to 19% determined by point counting). Albitized plagioclase and authigenic adularia on potassium feldspar grains may also occur. Clay cements are mainly composed of illite and some illite-smectite mixed-layer minerals. Other minor diagenetic cements may be present, such as dispersed pyrite or anatase and barite-filled fractures. Quartz overgrowths clearly predate the burial carbonate cements, but they postdate some early carbonate cements that sometimes occur as small relics between the detrital quartz grain and its overgrowth. Chronologic relationships between quartz overgrowth and authigenic feldspar are not well understood. Each has been observed predating the other. Total porosities in the studied Keuper sandstones range up to 13%.

## METHODS

Detrital quartz grains and their overgrowths were examined using CL and a scanning electron microscope (SEM) JEOL JSM 840. Carbon-coated thin sections were observed using a JEOL CDU 40 CL detector, an accelerating voltage of 25 kV, and a probe current of 6 nA. Some quartz-rich sandstones were examined with a Technosyn cold-cathode instrument operated at 18 kV. CL colors were also investigated using the hot-cathode system described by Ramseyer et al. (1989) at 30 keV. Luminescence photomicrographs were recorded on Fuji 1600 ASA film with 2–3 min exposures on the cold-cathode instrument, and on Ilford film on the SEM. CL spectra were recorded with a CL spectrometer on another JEOL JSM 840 SEM (Blanc et al. 1994). This system consists of a parabolic mirror, a silica window allowing the passage of UV emissions, a Jobin-Yvon H10.UV grating spectrometer, and a Hamamatsu R636 photomultiplier, which allows detection from 200 to 900 nm. The efficiency in the red part is only one-sixth the efficiency in the blue part of the recording spectrum. Peaks at 500 and 800 nm are present in all the recorded spectra; they resulted from equipment response and are not related to the material studied. The spectra presented in this study were not corrected for instrument response.

SIMS analyses were made on gold-coated thin sections with a Cameca IMS 3f ion probe. Mass spectra were obtained over a mass range of 1–140 to determine which elements were present in significant amounts. Quantitative peak intensities were obtained for the following elements and masses: H (1), Li (7), Na (23), Al (27), Si (29 and 30), K (39), Ti (47 and 49), Fe (54 and 56), and Mn (55). The negative primary O beam with 1–2 nA intensity was focused onto a 10 $\mu$m wide spot. The field aperture was 60 $\mu$m, and the mass resolution ($M/\Delta M$) was 400. The energy slit aperture was open to 20 V, and an energy filtering of $-60 \pm 10$ V was applied to minimize polyatomic ion intensities and isobaric interferences. A liquid-nitrogen trap was used to lower the background, especially for H. The electron multiplier was used in the counting mode. Counting rates ranged from 4600 to 18000 cps for $^{30}Si$. Analyses were made by peak jumping, with counting

times of 3 s for masses 1, 27, 29, 30, and 56 and of 5 s for the other masses. Switching time was 1 s. Each analysis included 14 measurement cycles over the different masses. Peak count rates for each element were normalized to $^{30}Si$ after each cycle and then converted into concentration by correcting the measured ratio by the ionization yield of each element, relative to Si, calculated in the applied energy window (Hinton 1990). Reported errors represent two standard deviations. Fe contents were determined from the 54/30 ratios because high 56/30 ratios suggested possible isobaric interferences on mass 56. Ti contents were determined from both 47/30 and 49/30 ratios to minimize the background effect on such small ratios. The ratio of H/Si was not converted into concentration because of a lack of ionization yield data. Energy filtering minimized the matrix effects (Shimizu and Hart 1982). The calculation using ionization yields did not offer the precision that could be expected from use of calibration curves, but, in the absence of well-known available standards, it allowed an estimation of concentration from the ion probe measurements.

Concentrations determined by ion probe were compared with those obtained for Al using a Cameca SX50 electron microprobe with 20 nA sample current, 15 kV voltage, and 100 s counting time. Detection limits ($2\sigma$ error) were found to be about 90 ppm. Figure 2 shows a good 1:1 correlation between Al concentrations determined using ion probe measurements with ion yield corrections and those determined using the electron microprobe. The two points not on the correlation line correspond to quartz with low and variable Al concentrations (as shown by standard deviations).

Ion images were obtained with a Cameca IMS 5f for seven masses: 7, 23, 24, 27, 28, 39, and 40. A 250 × 250 $\mu$m primary-beam scan was used to remove gold from a 300 × 300 $\mu$m field for at least 10 min.

Fluid-inclusion data were obtained for the quartz cement (Demars and Pagel 1994). Care was taken to select only primary fluid inclusions. Inclusions present at the grain-overgrowth boundary represent fluids of the first stage of cementation, but none of these inclusions were large enough to allow measurement (oxides and clays, also present at this interface, could hide inclusions). Suitable fluid inclusions were found within quartz overgrowths as isolated two-phase aqueous inclusions, generally 2–5 $\mu$m in size, although sometimes as large as 10 $\mu$m. Microthermometric measurements were made on 200–300 $\mu$m thick plates on a heating and cooling stage. Calibration curves were determined using synthetic inclusions and standard melting products. Because the inclusions were very small, phase transformations could not be easily observed. When homogenization was suspected to have occurred, the temperature was lowered a few degrees. The reappearance of a vapor bubble at this stage indicated that the homogenization temperature actually had not been reached, and the measurement was repeated. Measurement accuracy is ±0.3 °C for melting and ±3 °C for homogenization temperatures.

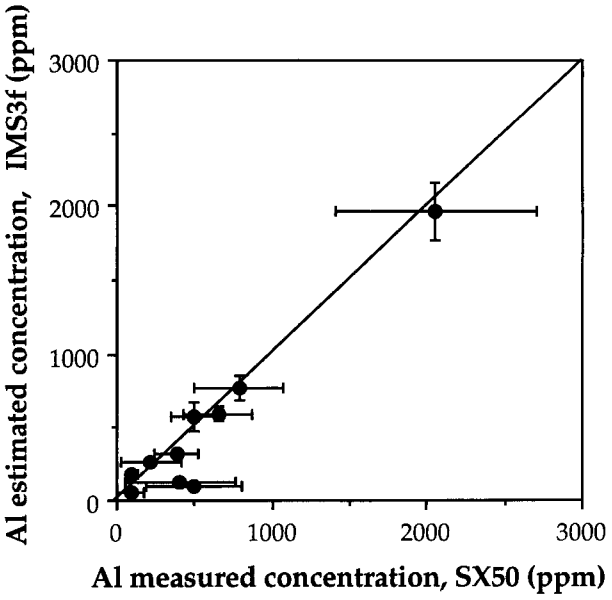


FIGURE 2. Comparison of Al concentrations deduced from IMS3f ion probe measurements and ion yields from Hinton (1990) and those measured by electron microprobe. Bars represent standard deviations.

## CATHODOLUMINESCENCE OF QUARTZ

### Cathodoluminescence petrography

**Occurrence of detrital and authigenic quartz.** Authigenic quartz occurs as euhedral overgrowths on detrital quartz grains or more rarely as small bipyramidal crystals filling pores. In images produced using the cold-cathode instrument, quartz overgrowths occur as dark areas around variously colored cathodoluminescent detrital grains. Images from the hot-cathode instrument described by Ramseyer et al. (1989) show dark blue cathodoluminescence in the cement but variable CL colors in detrital grains. If the equipment is attached to a SEM, the CL image of quartz is rather different because of a different detection system: Comparison of the crystal boundaries observed in BSE (backscattered electron) mode and the boundaries observed in CL mode emphasizes the presence of overgrowths around detrital quartz, but the CL equipment reveals quartz overgrowths occurring as bright areas around dull detrital quartz grains (Fig. 3). The distinction between bright overgrowths and darker detrital grains is thus easily and rapidly made. Silica cementation, therefore, was studied in various samples from each of the five selected boreholes.

**Detrital quartz grains.** The use of different CL instruments allows better definition of the boundaries and shapes of individual detrital grains. The widths of the detrital grains are reported in Table 1. Most of the detrital quartz grains have round shapes. Some moderately round grains were present in samples of borehole B3, whereas some rare angular grains were observed in the samples of borehole B8. Detrital grains do not show any interpene-

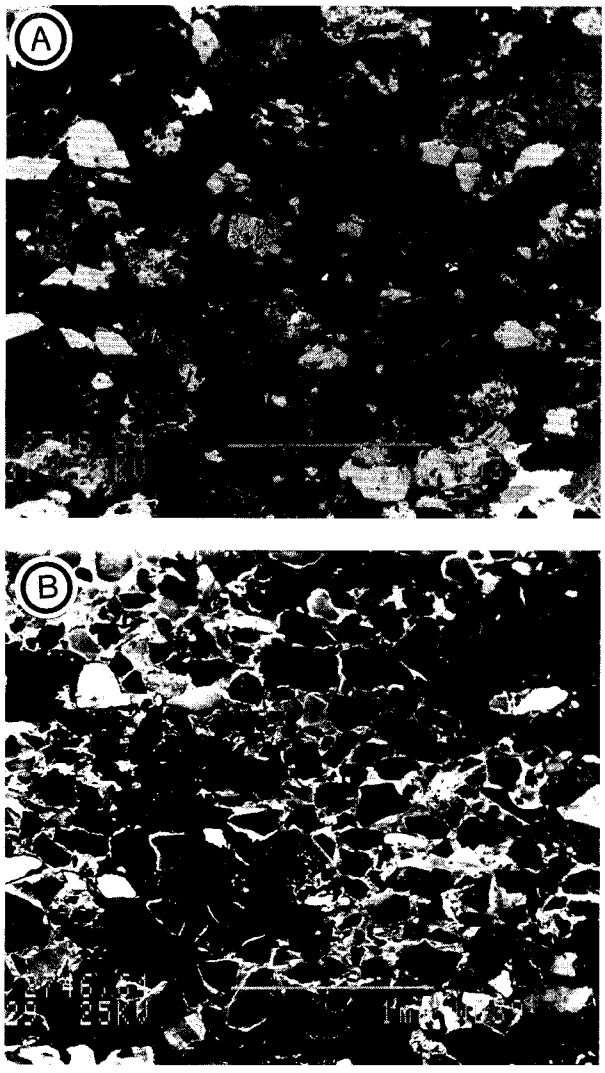


FIGURE 3. SEM photomicrograph of a sandstone from borehole B8. (A) Backscattered electron image showing dark gray quartz (Qz) and (B) CL image of the same area showing bright luminescent thin overgrowths around slightly luminescent detrital grains; note the floating grains.

tration figures. They are normally connected to their neighbors by only one point but are sometimes totally isolated. No quartz-filled fractures with CL similar to that of overgrowths were found. CL colors of detrital quartz grains observed using the Technosyn instrument are variable. Most of the grains have a brown or a violet-blue color, but some are only blue whereas other angular grains appear rose.

**Authigenic quartz overgrowths.** CL highlights the quartz overgrowths around detrital quartz grains in the samples of the five selected boreholes. The quartz overgrowths show various widths, as given in Table 1 for the different boreholes. The quartz overgrowths are extremely well developed in the porous sandstones of borehole B3, in the Rhaetian sandstones of borehole B9, and in samples of borehole B1. Overgrowths are widespread in samples from borehole B8. In samples from borehole B2, overgrowths are not homogeneously distributed. Quartz overgrowths are defined by bright areas using SEM, but careful observation shows inhomogeneous patterns (Fig. 4) as already reported by Hogg et al. (1992). These Cl figures were also observed using the hot-cathode equipment on the microscope: Patches of shades of blue are visible at the very beginning of electron bombardment (Ramseyer et al. 1989), becoming duller with time. Some of the luminescence patterns are similar to twinning patterns. Others show concentric areas of different shades of luminescence, which could be described as zoning. However, most of the overgrowth patterns are patchy, without any indication of concentric growth or twinning, and may reflect areas with lattice defects or crystallographic orientation.

TABLE 1. Widths of detrital quartz grains and quartz overgrowths from the Keuper sandstones of the Paris basin, determined using CL

| | Grain size (μm) | | Overgrowth widths (μm) | |
|---|---|---|---|---|
| Borehole | Min. | Max. | Min. | Max. |
| B1 | 100 | 300 | 20 | 80 |
| B2 | 50 | 200 | 5 | 30 |
| B3 | 200 | 600 | 20 | 100 |
| B8 | 35 | 300 | 10 | 60 |
| B9 | 100 | 300 | 20 | 60 |

### Cathodoluminescence spectra of quartz overgrowths

The locations of the analyzed areas are shown in Figure 5. CL spectra of quartz overgrowths, recorded at room temperature, are shown in Figure 6. The spectra are characterized by a broad band in the UV region, centered at 330–340 nm. There is a broad continuous distribution with a maximum intensity at ~640 nm. The asymmetry of the 330–340 nm and 640 nm bands suggests the presence of other bands, the positions of which were searched for by fitting the CL spectra in Gaussian peaks. The asymmetry of the 640 nm emission band suggests the presence of another band centered around 500 nm. The asymmetry of the 330–340 nm band suggests the presence of several bands. According to Remond et al. (1992) there are three possibilities: 380 nm, 400 nm, and domains ranging from 440 to 470 nm. Monochromatic photomicrographs were taken at different wavelengths. Bright overgrowths appear more intense at about 330 nm. CL spectra were also recorded for quartz overgrowths from sandstones of the Alwyn area (North Sea), which appear nonluminescent using CL-SEM. These spectra do not show the 330 nm peak.

CL intensity and color in quartz are affected by electron bombardment. CL images taken before and after irradiation, at room temperature, are different and depend on wavelength. The 630 nm peak is greatly increased under prolonged electron bombardment (several minutes), as can be seen in Figure 7, in which the indicated squares

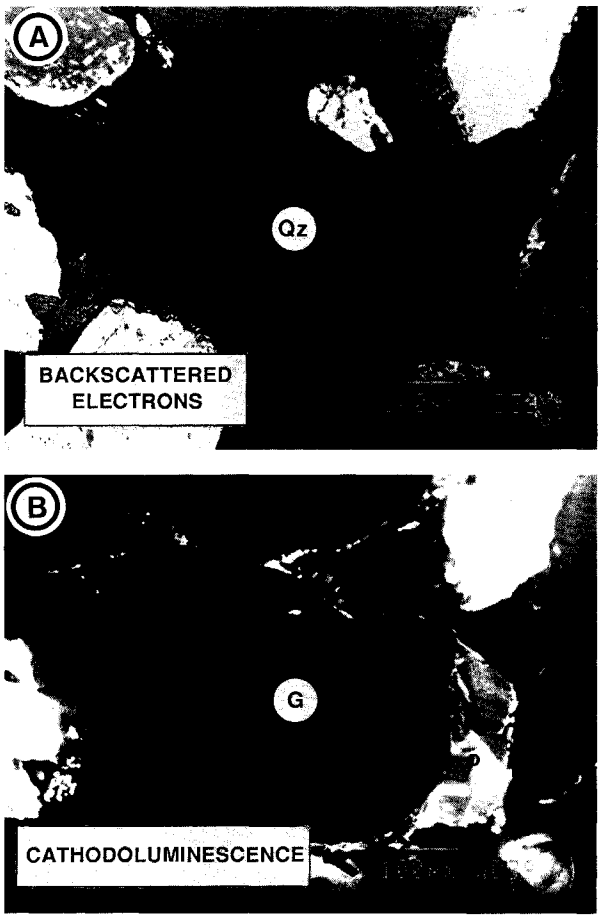


FIGURE 4. SEM photomicrograph of quartz from a Keuper sandstone from borehole B3. (A) Backscattered electron image showing the dark gray quartz (Qz) and (B) CL image of the same quartz showing the dark luminescent detrital grain (G) and the bright luminescent overgrowth (o); note the bright patterns in the overgrowth.

are areas irradiated for several minutes, whereas the 400 nm image remains unaffected (Fig. 7).

## TRACE ELEMENTS DETERMINED BY ION MICROPROBE, ELECTRON MICROPROBE, AND IONIC IMAGERY

On the basis of the patterns observed using CL, trace element profiles were determined across detrital quartz and areas of various CL intensities in quartz overgrowths. Variations of trace element abundances were measured with the ion probe and the electron probe for Al. The locations of the measurements are visible in Figure 5. Trace element contents, as well as $^{1}H/^{30}Si$ ratios, which were determined by ion probe measurements, are reported in Figure 8. The main differences between detrital quartz and overgrowths are Li and Al contents (Fig. 8). Al contents are much higher and more variable (up to 2100 ppm) in overgrowths than in detrital quartz. Despite its low concentration, Li content has the same characteristics as Al: It is low in detrital quartz and abundant

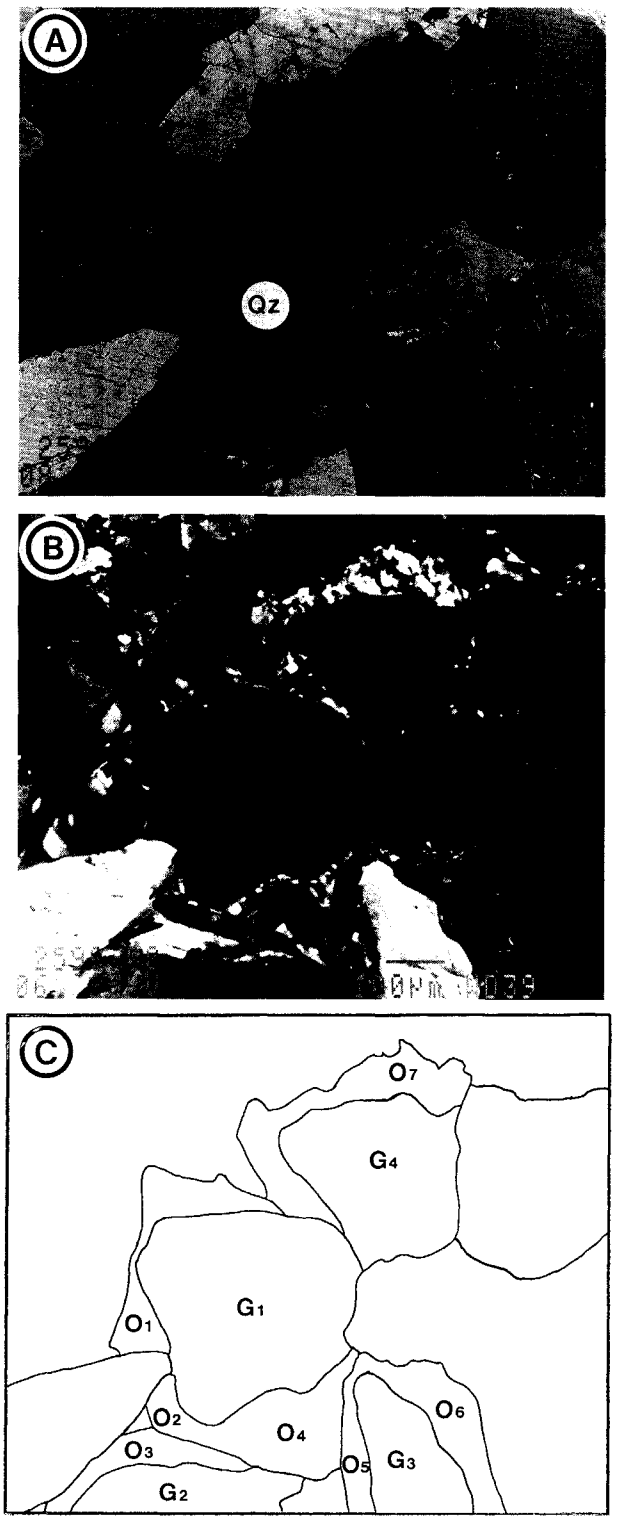


FIGURE 5. Authigenic quartz overgrown on detrital quartz grains in a Keuper sandstone from borehole B3. (A) Backscattered electron photomicrograph showing dark gray quartz (Qz), (B) CL photomicrograph, and (C) sketch of the analyzed locations in the overgrowths (O) and in the detrital grains (G).

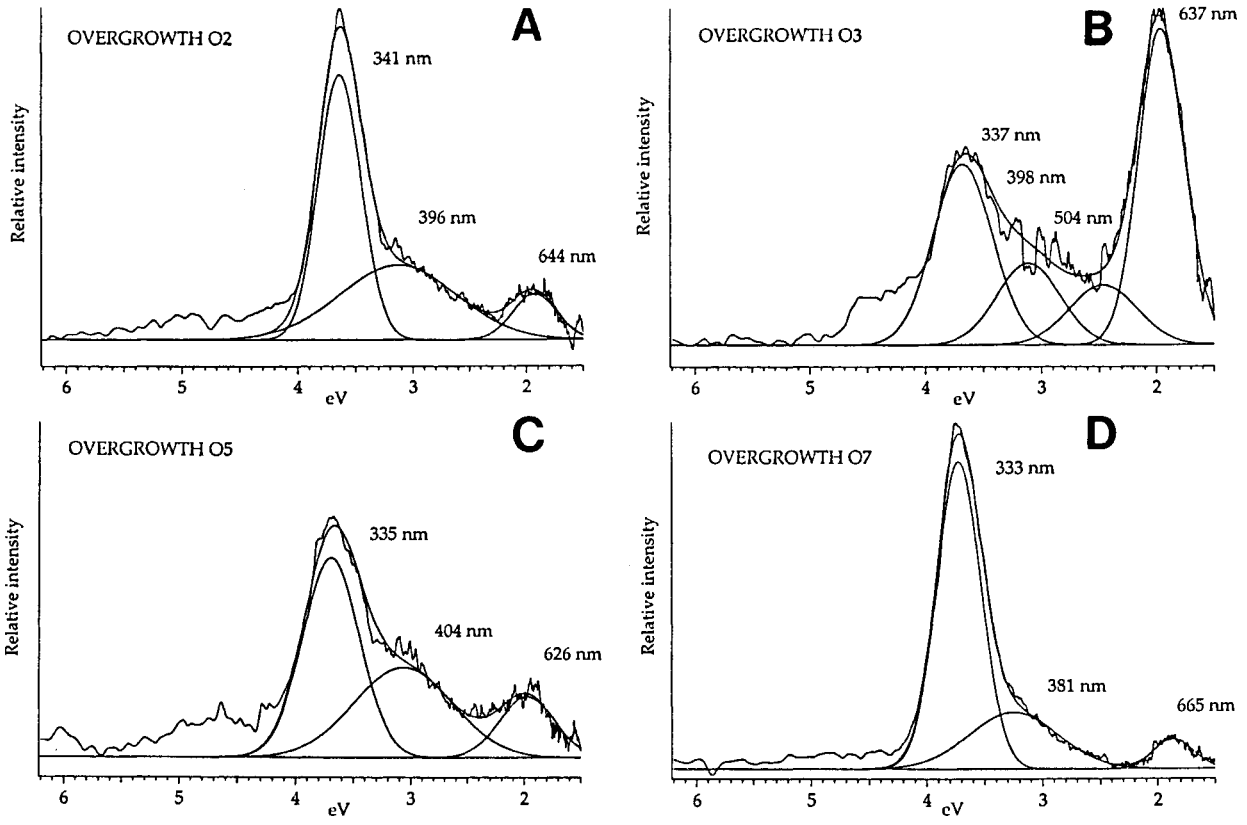


**FIGURE 6.** Cathodoluminescence spectra of some of the quartz overgrowths shown in Figure 5: (**A**) luminescent overgrowth O2, (**B**) bright luminescent overgrowth O3, (**C**) slightly luminescent overgrowth O5, and (**D**) very bright luminescent overgrowth O7.

in quartz overgrowths (up to 29 ppm). Bright overgrowths are characterized by the highest Al and Li contents. Figure 9 shows the correlation between Al and Li contents. Fe, Mn, K, Na, and H contents do not show any systematic difference between the detrital and the authigenic quartz (Fig. 8). Some detrital quartz may be enriched in Ti. K content is higher than Na content in some quartz. Such characteristics have already been observed in agates, K being incorporated with Al as a charge-compensating cation (Merino et al. 1995).

Electron microprobe measurements confirm the high Al contents in bright quartz overgrowths (Fig. 10). In detrital quartz grains, Al content is often lower than the detection limit (90 ppm) or may exceptionally reach about 300 ppm. In quartz overgrowths, minimum Al content is about 250 ppm, and maximum contents reach 2780 ppm. Profiles from core to border (or from border to core) revealed that no simple Al zonation exists for the different overgrowths (Fig. 10). This is consistent with the patchy variation in luminescence intensity noted previously.

SIMS images were acquired on a detrital quartz grain (G4 on Fig. 5) surrounded by a very bright luminescent overgrowth (O7 on Fig. 5). Figure 11 presents the Al and Li distribution over this area. High Li and Al contents were found within the brightly luminescent overgrowth. The distribution of the other elements measured (Na, Mg, K, Ca) did not show any correlation and is not presented.

For comparison, Al and Li contents were measured on detrital quartz grains and their overgrowths from sandstones of the Alwyn area (North Sea). The Li and Al contents were always higher in the overgrowth than in the detrital grain. However, Li and Al contents were much lower in nonluminescent quartz overgrowths from the Alwyn sandstones than in bright luminescent quartz overgrowths from Keuper sandstones of the Paris basin (Fig. 12).

## MICROTHERMOMETRIC RESULTS

The mean results of microthermometric measurements in quartz overgrowths are given in Table 2. Homogenization and melting temperatures were corrected according to the calibration curve established for the heating and cooling stage used for the measurements. The temperatures were obtained from samples from boreholes B1, B2, and B3 (Demars and Pagel 1994).

### Homogenization temperatures

Measured homogenization temperatures ($T_h$) are given in Table 2. Aqueous inclusions in borehole B3 homogenized between 75 and 122 °C. Inclusions in borehole B2

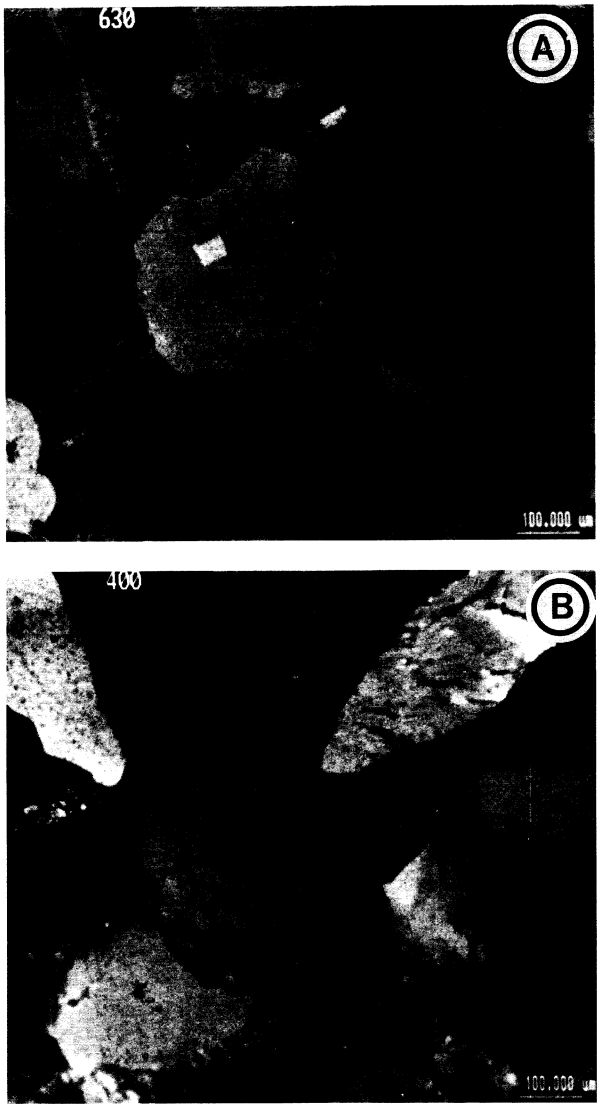


FIGURE 7. SEM photomicrograph of cathodoluminescence at various wavelengths. (**A**) At 630 nm, arrows show the location of prolonged electron bombardment. Note the higher cathodoluminescence signal of these areas. (**B**) At 400 nm, bombarded areas do not show any variation of the cathodoluminescence signal.

homogenized at higher temperatures ranging from 94 to 119 °C at greater depths. Inclusions in quartz overgrowths in borehole B1 homogenized at tightly constrained and higher temperatures ranging from 116 to 129 °C.

### Melting temperatures

Measured melting temperatures ($T_m$) in quartz overgrowths are given in Table 2. Corresponding salinities were calculated using the Bodnar (1993) equation. $T_m$ measured in quartz overgrowths from borehole B3 ranges from −15.5 to −1.7 °C (corresponding to salinities of 2.9–19 wt% NaCl eq.). In borehole B2, $T_m$ ranges from −18.4 to −7.9 °C (corresponding to salinities of 11.5–21.3 wt% NaCl eq.). In borehole B1, as $T_h$ exhibits a small dispersion, $T_m$ values are rather tightly grouped, ranging from −13 to −11.9 °C (corresponding to salinities of 15.9–16.9 wt% NaCl eq.).

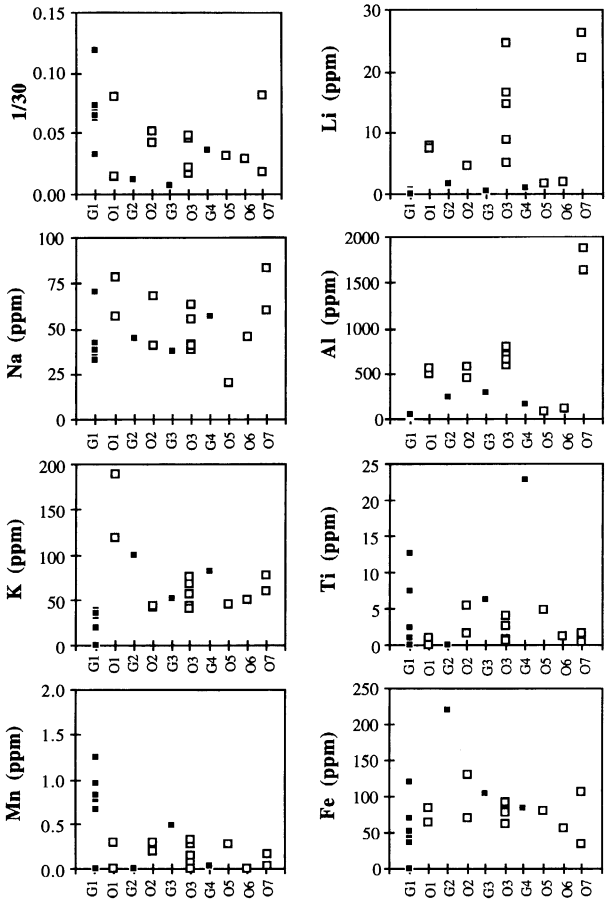


FIGURE 8. Trace element contents determined by ion probe for the various quartz areas shown in Figure 5. Contents are expressed in parts per million for all elements except H, for which the 1/30 ratio is used.

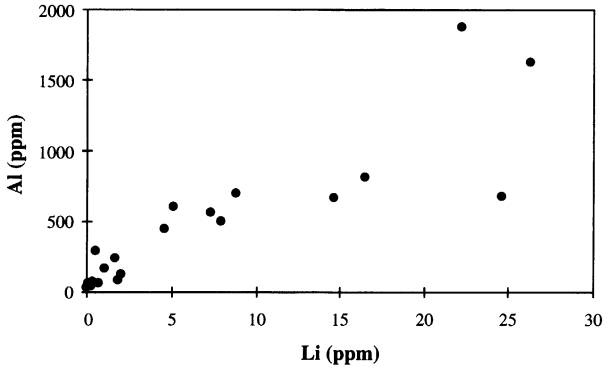


FIGURE 9. Plot of Al vs. Li contents of quartz determined by ion probe.

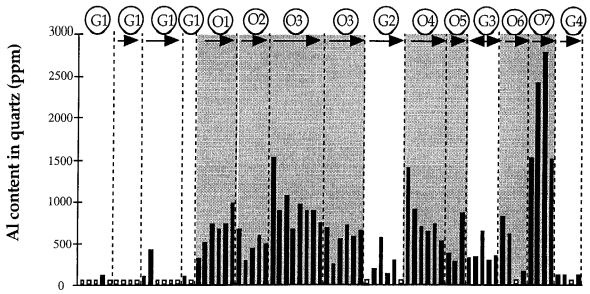


**FIGURE 10.** Al contents determined by electron probe of the various quartz areas shown in Figure 5. Arrows indicate growth directions, white histograms represent Al contents lower than the detection limit (90 ppm).

## INTERPRETATION AND DISCUSSION

### Cathodoluminescence spectrum of quartz overgrowths

Quartz overgrowths have often been reported as non-luminescent (Zinkernagel 1978) or dull luminescent. Ramseyer et al. (1988) reported common short-lived blue, blue-green, and bottle green luminescence colors in authigenic quartz overgrowths developed around detrital quartz grains in sandstones using a special CL optical microscope developed for investigation of low-luminescence intensities. The CL spectral investigation conducted between 200 and 900 nm on quartz overgrowths from the Keuper sandstones of the Paris basin revealed a major ubiquitous emission band in the UV range centered at about 330–340 nm. Such a band has never been reported in classical CL studies of quartz in sandstones, probably because many spectral studies were restricted to the visible range. Other CL peaks were noticed, but they are of minor importance. A high 650 nm peak was observed once but is probably related to intensity increase during continuous bombardment, which, as discussed above, is a normal process in this part of the spectra. The classification proposed by Zinkernagel (1978) does not take into account such quartz overgrowth spectra.

### Origin of CL in the UV range in the quartz overgrowths of the Paris basin: Possible correlations

Despite the extensive use of CL in geologic studies, the mechanisms responsible for it are not yet well understood. Studies linking doped synthetic crystals or geologic sample analyses with the recording of CL spectra and the observation of CL color have led to several hypotheses about the origin of visible CL. Ti, Ti/Fe ratio (Sprunt 1981), Mn (Marshall 1988), Al (Perny et al. 1992; Grant and White 1978), Na and Li (Perny et al. 1992), and $H_2O$ (Owen 1984) have been frequently mentioned as possible activators. Other authors dispute the possible influence of activators in quartz because of the general absence of CL zonations. However, some observations with appropriate equipment suggest that zonations may exist (Ramseyer and Mullis 1990). Zinkernagel (1978) concluded that the ordering degree of the quartz lattice is the cause of

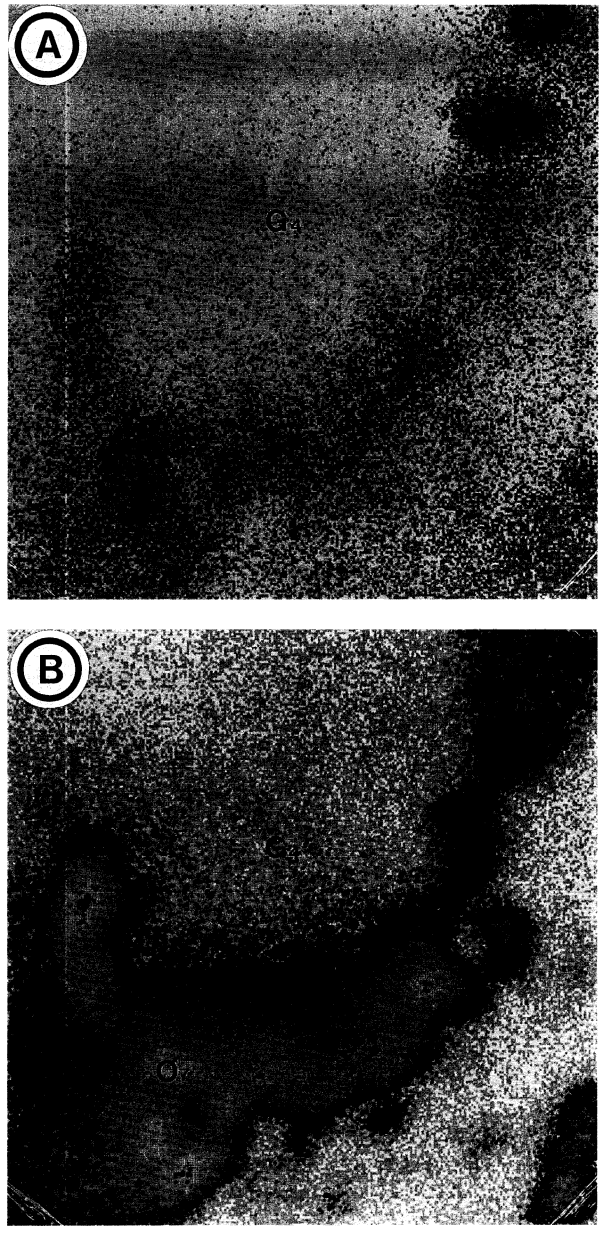


**FIGURE 11.** Ionic images of the area shown in Figure 5, including quartz grain G4 and overgrowth O7. (**A**) Li image: The highest signal is shown in the overgrowth O7 (black); (**B**) Al image: The highest signal is shown in the overgrowth O7 (dark gray). The ionic images are inverted in comparison with standard SEM photomicrographs.

CL. SIMS and electron microprobe analyses demonstrated that high Al and Li contents are mainly located in quartz overgrowths. The abundances of these two trace elements correlate strongly with the UV-CL brightness of the diagenetic quartz and therefore with the intensity of the 330–340 nm band. Electron microprobe analyses showed that Al concentrations varied from 250 to 2780 ppm in quartz overgrowths. The other trace elements an-

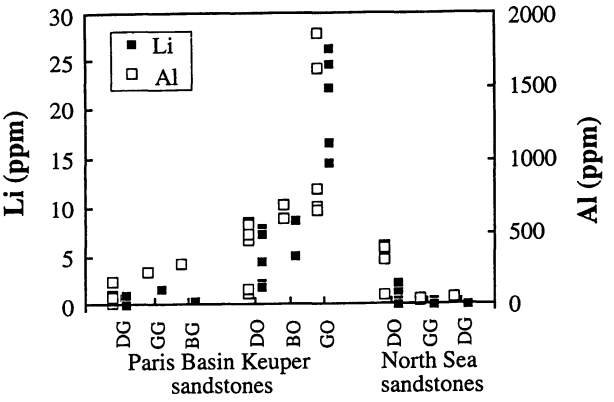


**FIGURE 12.** Al and Li contents of various detrital quartz grains and quartz overgrowths from Keuper sandstones of the Paris basin and from sandstones of the Alwyn area (North Sea). DG = dark grain, GG = gray grain, BG = bright grain, DO = dark overgrowth, GO = gray overgrowth, BO = bright overgrowth.

alyzed by means of SIMS (Na, K, Fe, Ti, Mn, and even Mg, Cl, and F) were either not correlated with the quartz overgrowth luminescence or had very low concentrations. Although Ti, Ti/Fe (Sprunt 1981), Mn (Marshall 1988), and $H_2O$ (Owen 1984) have been found to be potential activators of the quartz CL, they are not responsible for the observed UV-CL emission at 330–340 nm. OH has often been mentioned as a potential cause for some quartz CL peaks. However, H contents measured by ion probe do not correlate with the brightness of the overgrowths. Because H may be found at different locations ($4H^+$ for $Si^{4+}$ or $H^+ + Al^{3+}$ for $Si^{4+}$), the lack of correlation does not directly imply that OH is not involved in UV-CL emissions but suggests that it could not be the only source of luminescence. However, trace elements such as Al and Li appear to be of great importance in the 330–340 nm emission, as is shown by the similarity of the CL image of the very bright quartz overgrowth and the Li and Al images obtained with the ion probe. Al (or a specific cation-compensated Al point defect) has already been mentioned as a possible luminescence center of the short-lived CL by Perny et al. (1992). Grant and White (1978) also claimed that a 400–500 nm band may be associated with the replacement of Si by Al. Substitution of Al for Si is known to be the most important mechanism of compositional variation in quartz (Frondel 1962). Valence compensation is completed by the concomitant incorporation of $H^+$ and a small alkali ion, either Li or Na, or both (Frondel 1962), into interstitial positions. $Al^{3+}$ substitutes for $Si^{4+}$ in the Si-O tetrahedra, and the monovalent alkali ion, acting as charge compensator, is located in interstitial positions in channels that parallel the *c* axis (Jain and Nowick 1982). However, it is still unclear if concomitant Al-Li incorporation is directly or indirectly correlated with the intensity of the 330–340 nm band, i.e., do the trace elements act as activators or do the $(Al/Li^+)^0$ cause structural defects, such as lattice distortion, which enhance the intrinsic or self-activated luminescence? The $(Al/Li^+)^0$ point defect could be observed using electronic paramagnetic resonance (EPR) after irradiation to make this defect paramagnetic. Unfortunately, the studied quartz overgrowths are only a few micrometers wide and are difficult to separate from the host detrital quartz grain. Because no in situ EPR spectra could be obtained, the $(Al/Li^+)^0$ presence and its correlation with the UV emission of synthetic Li-doped quartz could not be observed. Whatever the mechanism may be, the coupled Al-Li substitution in the quartz overgrowths correlates with the UV emission at 330–340 nm.

## Depositional environments for development of such overgrowths

The 330–340 nm emission band in spectra of the quartz overgrowths from the Keuper sandstones of the Paris basin is absent from the spectra of quartz overgrowths from North Sea sandstones. A better knowledge of the growth conditions, in terms of thermometry and chemistry, was thought to be essential to define the most favorable environment for the development of such diagenetic quartz. The occurrence of UV emission in quartz overgrowths could therefore be related to a well-defined diagenetic environment.

Microthermometric data for quartz cements from the Keuper sandstones of the Paris basin provided homogenization temperatures for the fluid inclusions between 89 and 124 °C, depending on the depth and the location of the sample. With the assumption of a thermal gradient similar to that at present, it has been concluded that quartz cementation occurred at relatively great burial depths (Demars and Pagel 1994).

Salinities range from 2.9 to 21.3 wt% NaCl eq. Such moderate to high salinities have been related to variously

**TABLE 2.** Microthermometric results obtained for quartz overgrowths from the Keuper sandstones of the Paris basin (from Demars and Pagel 1994)

| Borehole | Depth (m) | N$T_h$ | $T_h$min (°C) | $T_h$max (°C) | Mean $T_h$ (°C) | N$T_m$ | $T_m$min (°C) | $T_m$max (°C) |
|---|---|---|---|---|---|---|---|---|
| B1 | 2756.07 | 3 | 119.0 | 124.0 | 122.0 ± 2.6 | 1 | — | — |
| B1 | 2781.81 | 24 | 116.0 | 129.0 | 123.6 ± 3.6 | 20 | −13.0 | −11.9 |
| B2 | 2805.50 | 18 | 94.0 | 119.4 | 107.6 ± 7.4 | 34 | −18.4 | −7.9 |
| B3 | 2598.00 | 25 | 74.9 | 121.7 | 91.7 ± 10.7 | 67 | −15.5 | −2.3 |
| B3 | 2619.38 | 15 | 86.4 | 93.4 | 88.9 ± 2.0 | 31 | −12.3 | −1.7 |
| B3 | 2624.50 | 2 | 93.0 | 94.5 | 93.7 ± 1.0 | 4 | −5.8 | −4.2 |

*Note:* $T_h$ = homogenization temperature, $T_m$ = melting temperature, and N = number of measurements.

diluted mixtures of primary and secondary brines, which probably originated from eastern Triassic evaporitic deposits (Matray et al. 1989; Demars and Pagel 1994). Quartz overgrowths from North Sea sandstones with dark CL have been found to have precipitated from lower salinity fluids (<4 wt% NaCl eq.) at about the same temperatures.

Li and Al occurrence in Keuper quartz overgrowths has been demonstrated to be a possible cause for the cathodoluminescence emission in the UV range. The high Li content in quartz could be explained by either rapid growth (Poty 1969) or growth from an Li-enriched fluid. The rarity of inclusions in any quartz overgrowth (regardless of the crystallographic direction) do not favor the hypothesis of rapidly grown quartz. Therefore, the most plausible option is that the fluids from which quartz precipitated were enriched in this ion. High Li values have been reported for saline solutions associated with oil fields in the Paris basin (Fontes and Matray 1993). These authors precluded the origin of Li from diagenetic reactions and concluded that the high content of trace elements, such as Li, in the solutions must be due to contributions from an extremely evolved primary brine. Diagenetic quartz enriched in Li should have precipitated from similar saline solutions. The 330–340 nm emission band seems, therefore, to be related to specific diagenetic conditions and in particular to the nature of the diagenetic fluid. The contribution of an extremely enriched primary brine has favored the precipitation of Al- and Li-enriched quartz, cathodoluminescent in the UV range.

## Acknowledgments

This study was funded by the oil companies Elf Aquitaine and Total and by the French Ministry for Research and Technology ("Etudes intégrées des bassins sédimentaires"). We thank Arnaud Meyer, Frédéric Sommer, and Frédéric Walgenwitz for providing the Paris basin samples, Ph. Karcher (Centre Géochimie de la Surface, Strasbourg) for technical assistance in SEM observations, J.M. Claude (Université Nancy I) for help with the electron microprobe measurements, and J.M. Luck (Université Sciences et Techniques du Languedoc, Montpellier) for providing the Cameca IMS5f. In situ measurements were made using the Cameca IMS3f at the Centre de Recherches Pétrographiques et Géochimiques, Nancy. We are indebted to K. Ramseyer (Bern Institute, Switzerland) for fruitful discussions and for critical reading of the manuscript. We are especially thankful to L. Reisberg (CRPG, Nancy) and N. Clauer (CGS, Strasbourg) for improving the manuscript.

## References cited

Bambauer, H.U. (1961) Spurenelementgehalte und γ-Farbzentren in Quarzen aus Zerrklüften der Sweizer Alpen. Schweizerische Mineralogische und Petrographische Mitteilungen, 41, 335–369.

Blanc, P., Arbey, F., Cesbron, F., Cros, P., and Ohnenstetter, D. (1994) L'utilité de la microscopie à balayage dans les travaux géologiques: L'exemple du sondage de Balazuc. Bulletin de la Societé Géologique de France, 165, 341–352.

Bodnar, R.J. (1993) Revised equation and table for determining the freezing point depression of $H_2O$-NaCl solutions. Geochimica et Cosmochimica Acta, 57, 683–684.

Burley, S.D., Mullis, J., and Matter, A. (1989) Timing diagenesis in the Tartan reservoir (UK North Sea): Constraints from combined cathodoluminescence microscopy and fluid inclusion studies. Marine and Petroleum Geology, 6, 98–120.

Demars, C., and Pagel, M. (1994) Paléotemperatures et paléosalinités dans les grès du Keuper du bassin de Paris: Inclusions fluides dans les mineraux authigènes. Comptes Rendus de l'Académie des Sciences de Paris, t 319, Série II, 427–434.

Fontes, J.C., and Matray, J.M. (1993) Geochemistry and origin of formation brines from Paris Basin, France: 2. Saline solutions associated with oil fields. Chemical Geology, 109, 177–200.

Frondel, C. (1962) The system of mineralogy: III. Silica minerals, 334 p. Wiley, New York.

Grant, P.R., and White, S.H. (1978) Cathodoluminescence and microstructure of quartz overgrowths on quartz. In O. Johari, Ed., Scanning electron microscopy, p. 789–794. Scanning Electron Microscopy, Chicago.

Guscott, S.C., and Burley, S.D. (1993) A systematic approach to reconstructing paleofluid evolution from fluid inclusions in authigenic quartz overgrowths. In Geofluids'93, 323–328.

Hanusiak, W.M. (1975) Low temperature cathodoluminescence of crystalline silica for use in the characterization of respirable dusts. M.Sc. thesis, Pennsylvania State University, State College.

Hinton, R.W. (1990) Ion microprobe trace element analysis of silicates: Measurement of multi-element glasses. Chemical Geology, 83, 11–25.

Hogg, A.J.C., Sellier, E., and Jourdan, A.J. (1992) Cathodoluminescence of quartz cements in Brent group sandstones, Alwyn South, UK North Sea. In Geology of the Brent Group, 61, 421–440.

Jain, H., and Nowick, A.S. (1982) Electrical conductivity of synthetic and natural quartz crystals. Journal of Applied Physics, 53, 447–484.

Marshall, D.J. (1988) Cathodoluminescence of geological materials, 146 p. Unwin Hyman, London.

Matray, J.M., Meunier, A., Thomas, M., and Fontes, J.C. (1989) Les eaux de formation du Trias et du Dogger du Bassin parisien: Histoire et effets diagénétiques sur les réservoirs. Bulletin des Centres de Recherche Exploration-Production de Elf-Aquitaine, 13/2, 483–504.

McBride, E.F. (1963) A classification of common sandstones. Journal of Sedimentary Petrology, 33, 664–669.

Merino, E., Wang, Y., and Deloule, E. (1995) Genesis of agates in flood basalts: Twisting of chalcedony fibers and trace element geochemistry, American Journal of Science, 295, 1156–1176.

Owen, M.R. (1984) Some phenomena associated with melting detrital quartz grains in the luminoscope. Nuclide Corporation Pub. 1090/0184.

Perny, B., Eberhardt, P., Ramseyer, K., Mullis, J., and Pankrath, R. (1992) Microdistribution of Al, Li, and Na in α quartz: Possible causes and correlation with short-lived cathodoluminescence. American Mineralogist, 77, 534–544.

Poty, B. (1969) La croissance des cristaux de quartz dans les filons sur l'exemble du filon de la Gardette (Bourg d'Oisans) et des filons du massif du Mont-Blanc, 162 p. Thesis, University of Nancy, France.

Ramseyer, K., Fischer, J., Matter, A., and Mullis, J. (1988) Cathodoluminescence colours of α quartz. Mineralogical Magazine, 52, 669–677.

Ramseyer, K., Fischer, J., Matter, A., Eberhardt, P., and Geiss, J. (1989) A cathodoluminescence microscope for low intensity luminescence. Journal of Sedimentary Petrology, 59, 619–622.

Ramseyer, K., and Mullis, J. (1990) Factors influencing short-lived blue cathodoluminescence of α-quartz. American Mineralogist, 75, 791–800.

Remond, G., Cesbron, F., Chapoulie, R., Onhenstetter, D., Roques-Carmes, C., and Schvoerer, M. (1992) Cathodoluminescence applied to the microcharacterization of mineral materials: A present status in experimentation and interpretation. Scanning Microscopy, 6, 23–68.

Ruppert, L.F., Cecil, C.B., and Stanton, R.W. (1985) Authigenic quartz in the Upper Freeport coal bed, west-central Pennsylvania. Journal of Sedimentary Petrology, 55, 334–339.

Shimizu, N., Semet, M.O., and Allègre, C. (1978) Geochemical applications of quantitative ion microprobe analysis. Geochimica et Cosmochimica Acta, 42, 1321–1334.

Shimizu, N., and Hart, S.R. (1982) Applications of the ion microprobe to geochemistry and cosmochemistry. Annual Review Earth and Planetary Sciences, 10, 483–526.

Sippel, R.F. (1968) Sandstone petrology, evidence from luminescence petrography. Journal of Sedimentary Petrology, 38, 530–554.

Smith, J.V., and Stenstrom, R.C. (1965) Electron-excited luminescence as a petrologic tool. Journal of Geology, 73, 627–635.

Smith J.V., and Steele, I.M. (1984) Chemical substitution in silica polymorphs. Neues Jahrbuch für Mineralogie Monatshefte, H3, 137–144.

Spötl, C., Matter, A., and Brévard, O. (1993) Diagenesis and porewater evolution in the Keuper reservoir, Paris Basin (France). Journal of Sedimentary Petrology, 63, 909–928.

Sprunt, E.S. (1981) Causes of quartz cathodoluminescence colors. In O. Johari, Ed., Scanning electron microscopy, p. 525–535. Scanning Electron Microscopy, Chicago.

Suttner, L.J., and Leininger, R.K. (1972) Comparison of the trace element content of plutonic, volcanic and metamorphic quartz from southwestern Montana. Bulletin of the Geological Society of America, 83, 1855–1862.

Zinkernagel, U. (1978) Cathodoluminescence of quartz and its application to sandstones petrology. Contribution to Sedimentology, 8, 69 p. E. Schweizerbart'sche Verlagsbuchhandlung, Stuttgart.

Manuscript received January 27, 1995
Manuscript accepted March 4, 1996